Open Access

Journal of Energy and Power Technology

LIDSEN Publishing Inc.

Original Research

Optimization of Heat Transfer in Parabolic Trough Collectors Using Advanced Turbulator Designs and Nanofluids

Mohsen Pourfallah, Ethan Languri *

Mechanical Engineering Department, Tennessee Tech University, Cookeville, TN, USA; E-Mails: mpourfall42@tntech.edu; elanguri@tntech.edu

* **Correspondence:** Ethan Languri; E-Mail: elanguri@tntech.edu

Academic Editor: Alfonso Chinnici

Journal of Energy and Power Technology
2025, volume 7, issue 1
doi:10.21926/jept.2501003

Received: October 19, 2024
Accepted: January 07, 2025
Published: January 15, 2025

Abstract

Parabolic trough collectors (PTCs) are essential for solar thermal energy systems, and their thermal efficiency can be significantly enhanced using turbulators and nanofluids. This numerical study introduces three novel fin-spiral turbulator configurations (4, 7, and 10 blades) to enhance heat transfer within the absorber tube. Additionally, three nanofluid types including water-based single-walled carbon nanotubes (SWCNT), cupric oxide (CuO), and a hybrid SWCNT-CuO, at concentrations of 1%, 3%, and 5% were evaluated. The simulations, conducted in ANSYS-FLUENT under steady-state turbulent flow conditions, revealed that the 10-blade turbulator improved the heat transfer coefficient by 12.25% compared to a plain tube, while the hybrid SWCNT-CuO/water nanofluid exhibited a 24.8% increase in thermal conductivity compared to the base fluid. Furthermore, a maximum pressure drop increase of 44% was observed for the hybrid nanofluid at 5% volume concentration and a Reynolds number of 12,500. The study also demonstrated that the Performance Evaluation Criterion (PEC) improved by 15.6% for the hybrid nanofluid compared to CuO/water nanofluid. These findings highlight the effectiveness of combining fin-spiral turbulators and hybrid nanofluids to optimize the thermal and hydraulic performance of PTC systems.

Keywords
Parabolic trough collector (PTC); turbulator; single wall carbon nanotubes (SWCNT); hybrid nanofluids; thermal performance

1. Introduction

Renewable energy is essential in combating the growing challenges of climate change, providing a sustainable and eco-friendly alternative to conventional fossil fuels. The significance of renewable energy lies in its ability to harness naturally occurring and renewable sources such as solar energy [1], wind power [2], and tidal forces [3], minimizing the ecological impact associated with traditional energy production. Solar energy, a cornerstone of sustainable power, is employed through both electrical and thermal applications, showcasing its versatility in meeting diverse energy needs. Photovoltaic (PV) cells convert solar energy directly into electricity for electrical applications. This technology has seen remarkable advancements, resulting in increased efficiency and cost-effectiveness [4]. On the other hand, in thermal applications, solar energy is employed to generate heat for different purposes such as space heating [5], liquid heating [6], and industrial operations [7-10]. Parabolic trough collectors (PTCs) are very prevalent for power and heat production of residential areas. The improvement of thermal performance in PTCs directly impacts reliability, cost, and overall productivity. Researchers use various techniques to increase the heat absorption from solar radiation and reduce heat dissipation to the environment. Among the different active and passive technologies, using nanofluids and turbulators seems to be the most efficient way to enhance the convection heat transfer coefficient inside the heat transfer tube [11]. Each approach has its disadvantages and limitations such as increasing the pressure drop, sedimentation, and economic feasibility. Therefore, more research and studies must be conducted by scholars on the hydrothermal characteristics of PTCs.

Inefficient heat absorption by working fluids results in a low conversion efficiency of solar radiation into thermal energy. Therefore, optimizing the hydrothermal properties of heat transfer fluids is crucial for developing cost-effective and high-efficiency solar collectors. Nanofluid technology has opened a new window to provide enhanced thermophysical properties for fluids flowing inside the solar collector tubes [12]. The ability of nanofluids to enhance the performance of solar thermal systems depends on various factors, including their thermal conductivity, density, viscosity, specific heat, and optical properties for absorbing solar radiation [13]. Mashhadian et al. [14] utilized a hybrid nanofluid consisting of Al_2O_3-MWCNT/water to analyze the effect of the concentrations of the hybrid nanofluid ranging from 0.01% to 0.04% on the performance of direct-absorbing PTC. Their experimental findings revealed that the hybrid nanofluid outperformed the single nanofluid in terms of optical properties. They concluded that using hybrid nanofluids led to a 197% improvement in the thermal efficiency of the solar collector. Two different hybrid nanofluids including Al_2O_3-SiO_2/water and Al_2O_3-CuO/water were applied to increase the thermal performance in a PTC by Abdulhaleem et al. [15]. They employed the Tow-phase Mixture model to explain the impact of Reynolds number and nanofluids concentration on Nusselt number, pressure drop, and performance coefficient. It is indicated that the maximum 47% increment of the Nusselt number was achieved by Al_2O_3 (0.25%)-CuO (0.75%)/water while this value was decreased by 33% for

another hybrid nanofluid at the same volume fraction. Dou et al. [16] introduced two synthetic oils encompassing Therminol VP1 and Syltherm 800 besides copper as novel nanoparticles in a basic parabolic solar collector. They examined various inlet temperatures and velocities at volume fractions of 1%, 3%, and 5% to determine optimal hydrothermal performance. Their findings indicated that the syltherm 800 enhanced the convection heat transfer coefficient by 21.79%~19.73% at an inlet temperature of 600 K and volume fraction of 3% while this value was 15.29%~11.67% within a velocity range between 0.1 to 3.5 m/s. While researchers have recommended enhancing heat transfer fluid thermal properties with nanofluids, they have also put forward alternative modifications to improve the efficiency of the solar collector system [17-20]. These alterations primarily focus on the system's geometry, involving morphological adjustments to enhance the heat transfer of nanofluids.

Sheikholeslami et al. [21] introduced a novel spiral turbulator aimed at enhancing the thermal efficiency of solar systems. They claimed that the turbulator both increased the swirl ratio and extended the heat transfer surface. So, their results showed that the rotational flow boosted with an increasing spiral rotation of the tape, consequently leading to a higher pressure drop. The friction factor and Nu exhibit increments of approximately 271.36% and 5.83%, respectively, with the rise in spiral rotation. Moreover, an increase in Reynolds number (Re) results in a 75.22% enhancement in Nu but concurrently induces a 12.43% reduction in the friction factor. Semi-circular and teardrop-shaped turbulators were added to the circular tube by Fang et al. [22]. Their finding indicated that these turbulators significantly influence heat transfer and friction coefficient. The heat transfer values reached a maximum of 257% and 298% higher for semi-circular and teardrop-shaped turbulators, respectively, compared to a standard plain tube. Babapour et al. [23] conducted research focused on improving thermal characteristics in a PTC. To achieve this objective, they employed a helically corrugated tube as the absorber, introducing modifications to its shape, including adjusting the pitch. The findings indicated an enhancement in the system's thermal performance of up to 2%. Al-Aloosi et al. [24] integrated circular, elliptical, and square fins of varying cross-sections and heights into the absorber tube of a parabolic trough collector. Numerical findings indicated that the highest thermal performance was achieved with circular, elliptical, and square fins, achieving values of 1.4, 1.31, and 1.26 respectively at Re = 4000. Additionally, there is a substantial increase in Nu, almost 51%, when transitioning from Re = 4000 to Re = 8000 for the square cross-section. Semi-spherical inner surfaces [25], dimpled tubes [26], and wavy surfaces [27] are other configurations of the turbulator used in solar thermal collectors. Using turbulators and nanofluids simultaneously paved a new way for scholars to take advantage of both methods and compensate for the disadvantages of each approach. The finned turbulator and perforated twisted tape were analyzed numerically with MWCNT-Al_2O_3/water as a hybrid nanofluid by Tavakoli and Soufivand [28]. They revealed that the maximum total entropy generation of 40.75% was achieved by a perforated twisted tape at Reynolds number of 30,000 and $\varphi = 3\%$. Similarly, the shift from a finned turbulator to a perforated tape turbulator resulted in a maximum efficiency change of 1.62% at Reynolds number 20,000 and $\varphi = 0\%$. Bellos et al. [29] suggested employing nanofluids based on oil with a 6% concentration of CuO, and they contrasted this with the conventional fins employed in the absorber. They also investigated the combined application of these techniques, finding that the nanofluids led to a 0.76% improvement in thermal efficiency. The incorporation of internal fins resulted in a 1.10% increase, while the combined techniques yielded a 1.54% enhancement in PTC thermal efficiency according to their study. Khetib et al. [30] enhanced energy and exergy

efficiencies in parabolic solar collectors by employing twisted turbulators and MgO-Cu/water nanofluids. They evaluated the average Nusselt number and pressure drop across Reynolds numbers ranging from 8000 to 32000, with nanofluid concentrations varying between 1% and 3%. The study concluded that changing the Reynolds number from 8000 to 32000 resulted in maximum improvements of 23.79% and 21.15% in energy and exergy efficiencies, respectively. The numerical study by Alnaqi et al. [31] investigated the hydrothermal impacts of twisted tape inserts in parabolic trough collectors (PTCs), utilizing MgO-MWCNT/thermal oil as a hybrid nanofluid for heat transfer. The MgO/MWCNT ratio was 80:20, and the volume fraction ranged from 0.25% to 2%. Their findings indicated that the performance evaluation criterion (PEC) using the LCRW model increased with rising Reynolds number up to 10,000 and then decreased up to 100,000 under all tested conditions.

Recent research has predominantly focused on nanofluids due to their superior thermal properties and potential to enhance heat transfer in solar thermal systems. However, the application of turbulators to improve the thermal performance of solar collectors remains underexplored. Moreover, the combined use of nanofluids and turbulators, a promising synergy for optimizing heat transfer and efficiency, has received limited attention in the existing literature. To address this research gap, this study introduces a novel hybrid approach that simultaneously leverages three configurations of fin-spiral turbulators (4, 7, and 10 blades) and water-based nanofluids, including single-walled carbon nanotubes (SWCNT), cupric oxide (CuO), and a hybrid SWCNT-CuO composition. The turbulent flow is simulated using the Standard K-ε model, while empirical correlations are applied to accurately derive key thermophysical properties such as density, viscosity, thermal conductivity, and specific heat for both single and hybrid nanofluids.

The key contributions of this study are twofold: first, the innovative combination of fin-spiral turbulators and hybrid nanofluids to achieve enhanced thermal performance in parabolic trough collectors (PTCs), and second, the comprehensive evaluation of heat transfer coefficients, pressure drops, and performance evaluation criteria (PEC) across different configurations and nanofluid types. The structure of this paper is as follows: Section 2 details the PTC model and geometric configurations; Section 3 validates the numerical model; Section 4 examines the thermal and hydraulic performance of the PTC, including the effects of nanofluid type and turbulator configuration; and finally, Section 5 highlights the major findings and implications of this study.

2. Model Description and Geometry

The absorber tube modeled in this study refers to a parabolic trough collector prototype in Spain introduced by Wirz et al. [32]. The original one includes a hollow absorber tube and a glass envelope, but in this study, three different types of fin-spiral turbulators are inserted in the center of the absorber tube. Figure 1 and Table 1 show the general view of the absorber tube and 4, 7, and 10-blade turbulators.

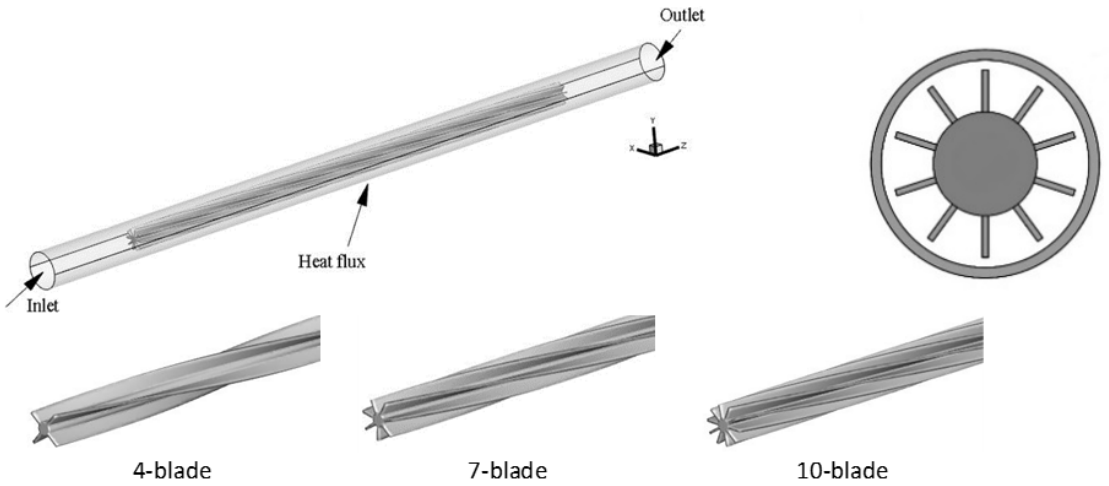

Figure 1 Overall view of the PTC with fin-spiral turbulator and three different tabulators.

Table 1 Geometrical parameters.

Characteristic	Sizes (mm)
Length (Tube)	4096
Diameter (Tube)	70
Length (Tape)	3000
Diameter (Turbulator)	50
Thickness (Turbulator)	1.3

3. Numerical Model

The governing equations and boundary conditions in this study are determined by solving the Reynolds-averaged Navier-Stokes equations. The ANSYS FLUENT, a finite-volume-based commercial CFD software is employed for numerical simulation. The Standard k-ε model is employed in this study to simulate turbulent flow inside the tube. The uniform velocity is considered for the inlet boundary, ranging from 0.07 m/s to 0.17 m/s, corresponding to Reynolds numbers between 5000 and 12500. The inlet temperature is assumed constant at 300 K. The tube outlet is characterized by a pressure-outlet boundary condition, while the outer surface of the absorber tube experiences variable heat flux based on the angle, as described by Eq. 1 [33]. All constant coefficients used in Eq. 1 are outlined in Table 2. The UDF (User Defined Function) is employed to introduce the variable heat flux to Fluent.

Table 2 Constant coefficient of variable heat flux equation [33].

$\boldsymbol{\theta}$	$0° \leq \theta < 18°$	$18° \leq \theta < 94°$	$94° \leq \theta \leq 180°$
ω	0	4.412×10^{-2}	4.237×10^{-2}
$\boldsymbol{a_0}$	300	3.146×10^{4}	3.363×10^{4}
$\boldsymbol{a_1}$	0	-8.090×10^{3}	-1.162×10^{4}
$\boldsymbol{b_1}$	0	-3.123×10^{4}	-1.899×10^{4}
$\boldsymbol{a_2}$	0	-7.178×10^{3}	3.648×10^{3}
$\boldsymbol{b_2}$	0	-3.119×10^{3}	7.571×10^{3}

The use of a double-precision pressure-based solver ensures enhanced accuracy and convergence in the numerical calculations. The PRESTO scheme is applied for pressure interpolation, while the QUICK scheme is employed for turbulence kinetic energy equations. The pressure-velocity coupling is handled using the SIMPLEC algorithm. Convective terms in the energy and momentum equations are discretized using a second-order upwind scheme for improved precision, whereas the specific dissipation rate term is interpolated using a first-order upwind scheme to balance accuracy and computational efficiency. Convergence is considered achieved when residuals for continuity and momentum equations are below 10^{-6}, and for the energy equation, below 10^{-9}.

$$q = a_0 + a_1 \cos(\omega\theta) + b_1 \sin(\omega\theta) + a_2 \cos(2\omega\theta) + b_2 \sin(2\omega\theta) \quad (1)$$

3.1 Governing Equation

This study considers the general governing equations for steady, three-dimensional, and incompressible flow, outlined as follows [34]:

Continuity equation:

$$\frac{\partial}{\partial x_i}(\rho u_i) = 0 \quad (2)$$

Momentum equation:

$$\frac{\partial}{\partial x_i}(\rho u_i u_i) = -\frac{\partial p}{\partial x_i} + \frac{\partial}{\partial x_j}\left[(\mu + \mu_t)\left(\frac{\partial u_i}{\partial x_j} + \frac{\partial u_j}{\partial x_i}\right) - \frac{2}{3}(\mu + \mu_t)\frac{\partial u_l}{\partial x_l}\delta_{ij}\right] \quad (3)$$

Energy equation:

$$\frac{\partial}{\partial x_i}\left(\rho c_p u_i T\right) = \frac{\partial}{\partial x_i}\left[\left(\lambda + \frac{c_p \mu_t}{\sigma_t}\right)\frac{\partial T}{\partial x_i}\right] + S_r \quad (4)$$

The Standard k-ε model is utilized to simulate the turbulent flow domain in this paper, which can be written as [35]:

k equation:

$$\frac{\partial}{\partial x_i}(\rho u_i k) = \frac{\partial}{\partial x_i}\left[\left(\mu + \frac{\mu_t}{\sigma_k}\right)\frac{\partial k}{\partial x_i}\right] + P_k - \rho\varepsilon \quad (5)$$

ε equation:

$$\frac{\partial}{\partial x_i}(\rho u_i \varepsilon) = \frac{\partial}{\partial x_i}\left[\left(\mu + \frac{\mu_t}{\sigma_\varepsilon}\right)\frac{\partial \varepsilon}{\partial x_i}\right] + C_{\varepsilon 1}\frac{\varepsilon}{k}P_k - C_{\varepsilon 2}\rho\frac{\varepsilon^2}{k} \quad (6)$$

The turbulent viscosity μ_t and production rate of k (P_k) are calculated:

$$\mu_t = C_\mu \rho \frac{k^2}{\varepsilon} \quad (7)$$

$$P_k = \mu_t \frac{\partial u_i}{\partial x_j}\left(\frac{\partial u_i}{\partial x_j} + \frac{\partial u_j}{\partial x_i}\right) \tag{8}$$

The standard constant used in this simulation: $C_\mu = 0.09, C_{\varepsilon 1} = 1.44, C_{\varepsilon 2} = 1.92, \sigma_k = 1.0, \sigma_\varepsilon = 1.3$, and $\sigma_t = 0.85$ [35].

The average Reynolds and average Nusselt numbers for nanofluid and hybrid nanofluid are defined as follows:

$$Nu = \frac{hD}{k_{nf\ or\ hnf}} \tag{9}$$

$$Re = \frac{\rho_{nf\ or\ hnf}\, uD}{\mu_{nf\ or\ hnf}} \tag{10}$$

Also, the friction factor and performance evaluation criteria (PEC) are calculated by following relations [17]:

$$f = \frac{\Delta P}{\frac{1}{2}\frac{L}{D}\rho u^2} \tag{11}$$

$$PEC = \frac{Nu_{nf\ or\ hnf}/Nu_f}{\left(f_{nf\ or\ hnf}/f_f\right)^{\frac{1}{3}}} \tag{12}$$

3.2 Thermophysical Characteristics of Nanofluids and Hybrid Nanofluids

This study adopts the single-phase model to characterize nanofluids and hybrid nanofluids comprising CuO and SWCNT nanoparticles. This is due to its validation for volume fractions below 10% and nanoparticle diameters under 100 nm [36]. The hydrothermal correlations of hybrid nanofluid including density, viscosity, specific heat, and thermal conductivity are calculated by the formulas shown in Table 3 [37]. The thermophysical properties of water, CuO, and SWCNT have been indicated in Table 4. The nanoparticles are assumed to be spherical, monodisperse, and uniformly dispersed in the base fluid. Thermophysical correlations are compiled into UDF code for introducing nanofluids and hybrid nanofluids into FLUENT.

Table 3 Hybrid nanofluid correlations [37].

Properties	**Hybrid Nanofluid**
Viscosity	$\mu_{hnf} = \frac{\mu_f}{(1-\varphi_1)^{2.5}(1-\varphi_2)^{2.5}}$
Density	$\rho_{hnf} = \rho_f(1-\varphi_2)\left((1-\varphi_1) + \varphi_1(\frac{\rho_{s1}}{\rho_f})\right) + \varphi_2\rho_{s2}$
Specific heat	$(\rho c_p)_{hnf} = (\rho c_p)_f(1-\varphi_2)((1-\varphi_1) + \varphi_1\frac{(\rho c_p)_{s1}}{(\rho c_p)_f}) + \varphi_2(\rho c_p)_{s2}$

Thermal conductivity	$\frac{\lambda_{hnf}}{\lambda_{bf}} = \frac{1-\varphi_2+2\varphi_2\left(\frac{\lambda_{s2}}{\lambda_{s2}-\lambda_{bf}}\right)\ln\left(\frac{\lambda_{s2}+\lambda_{bf}}{2\lambda_{bf}}\right)}{1-\varphi_2+2\varphi_2\left(\frac{\lambda_{s2}}{\lambda_{s2}-\lambda_{bf}}\right)\ln\left(\frac{\lambda_{s2}+\lambda_{bf}}{2\lambda_{bf}}\right)}$ $\frac{\lambda_{bf}}{\lambda_f} = \frac{1-\varphi_1+2\varphi_1\left(\frac{\lambda_{s1}}{\lambda_{s1}-\lambda_f}\right)\ln\left(\frac{\lambda_{s1}+\lambda_f}{2\lambda_f}\right)}{1-\varphi_1+2\varphi_1\left(\frac{\lambda_{s1}}{\lambda_{s1}-\lambda_f}\right)\ln\left(\frac{\lambda_{s1}+\lambda_f}{2\lambda_f}\right)}$

Table 4 Base fluid and nanoparticles characteristics.

Materials	Density (kg/m³)	Viscosity (N·s/m²)	Specific heat (J/kg·K)	Thermal conductivity (W/m·K)
Water	998	0.001	4182	0.613
CuO	6320	-	531.8	76.5
SWCNT	1400	-	1380	3500

3.3 Mesh Independency Analysis

The grid study aims to identify an appropriate grid resolution that ensures the number of grid points utilized does not influence the results. To achieve this, the Average Nusselt Number (ANU) is computed for various grid resolutions corresponding to the geometries with a 7-blad turbulator at Reynolds number (Re) of 5,000 with base working fluid (ϕ = 0%). As seen in Table 5, by analyzing the percentage error in ANU values between four grids, it is determined that grid number 519048 is suitable for the following simulations. Figure 2 illustrates the grids employed for the tube and turbulator.

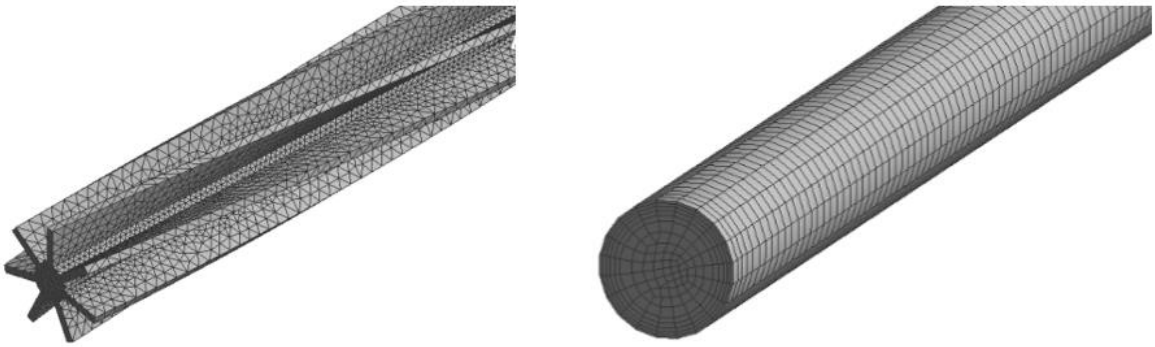

Figure 2 Mesh configuration for tube and turbulator.

Table 5 Error percentage of ANU at various mesh resolutions.

No. of grid cell	Error% (ANU)
162376	21.4%
342193	8.6%
519048	2.04%
748862	1.52%

3.4 Validation Study

The numerical results in this study were validated by comparing the experimental outlet temperature of synthetic thermal oil with the numerically calculated average Nusselt number for Syltherm-800 flow. As shown in Figure 3, the numerical outlet temperature from the absorber tube in the parabolic trough collector (PTC) demonstrates excellent agreement with experimental data reported by Zou et al. [38], who measured solar radiation intensity, fluid outlet temperature, and fluid flow rate at various daylight times. The maximum error observed in this validation study was 5.31%. Additional verification was performed using numerical results presented by Zhu et al. [39], based on a similar absorber tube configuration. Discrepancies due to differences in mesh density and solution procedures resulted in a maximum error of 4.05%, as shown in Figure 4. Overall, these validation results confirm the reliability and accuracy of the present numerical model for subsequent simulations.

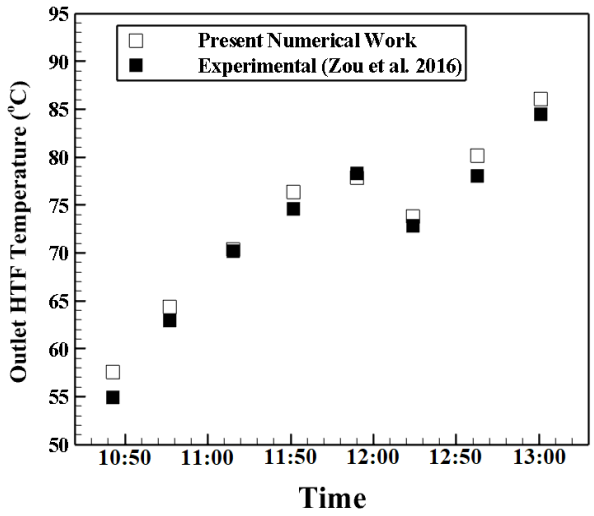

Figure 3 Validation of present outlet HTF temperature and experimental results by Zou et al. [38].

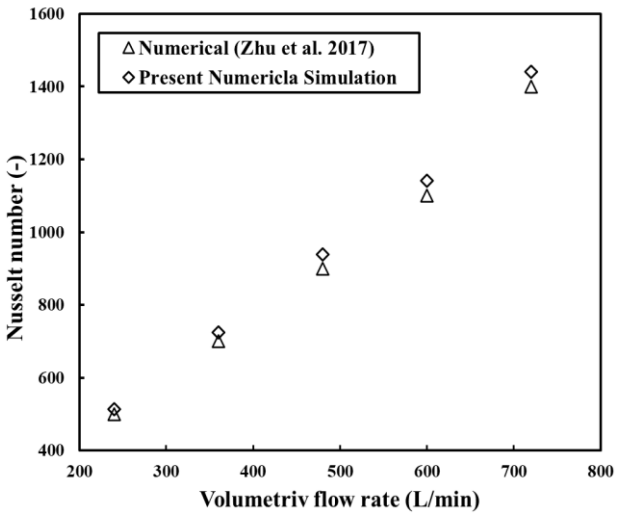

Figure 4 Validation of present numerical and numerical results by Zhu et al. [39].

4. Results and Discussion

This section explores the effects of three turbulator configurations on PTC's hydrothermal performance, including heat transfer coefficient, pressure drop, and PEC. Additionally, it investigates the effects of single-walled carbon nanotubes (SWCNT), cupric oxide (CuO), and a hybrid SWCNT-CuO. Simulations were conducted over Reynolds numbers ranging from 5000 to 12500.

4.1 The Effect of Turbulator Configurations

Figure 5 illustrates the variations in the heat transfer coefficient for the absorber tube flow concerning the Reynolds number across various turbulator configurations. Generally, there's a positive correlation between the heat transfer coefficient and the Reynolds number. Introducing turbulator blades notably enhances the convection heat transfer coefficient. Specifically, at a Reynolds number of 12,500, the absorber tube with 10 blades exhibits the highest heat transfer coefficient, showing a significant 12.25% increase compared to the configuration without a turbulator. Similarly, the configuration with 4 blades experiences a substantial 13.7% enhancement in the heat transfer coefficient.

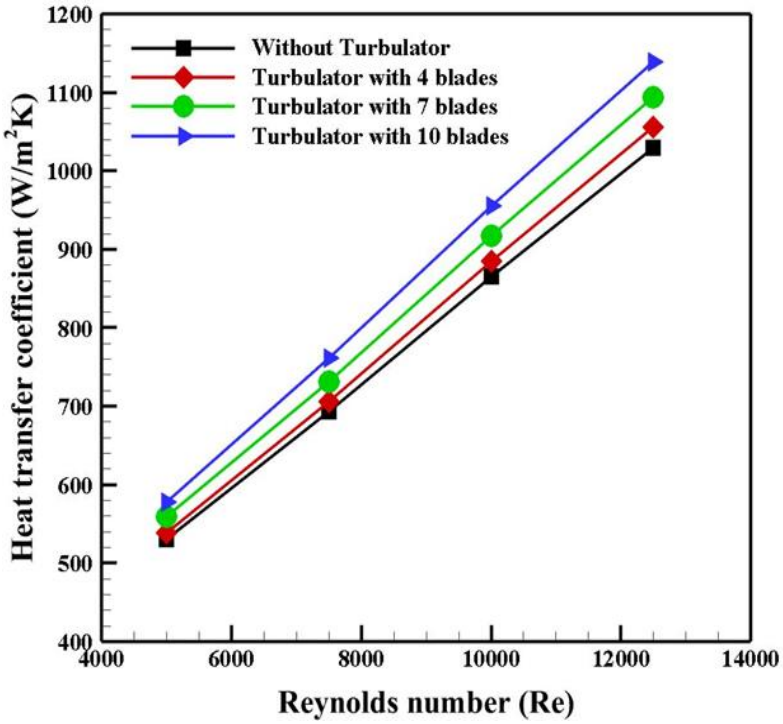

Figure 5 Heat transfer coefficient versus Reynolds number for different turbulators.

Figure 6 shows the outlet temperature of the three different configurations of the tabulator and plain tube. The outlet temperature decreases monotonically as the Reynolds number increases for all configurations. The outlet temperature increased with an increase in the number of blades at constant Reynolds numbers, owing to higher heat transfer coefficients.

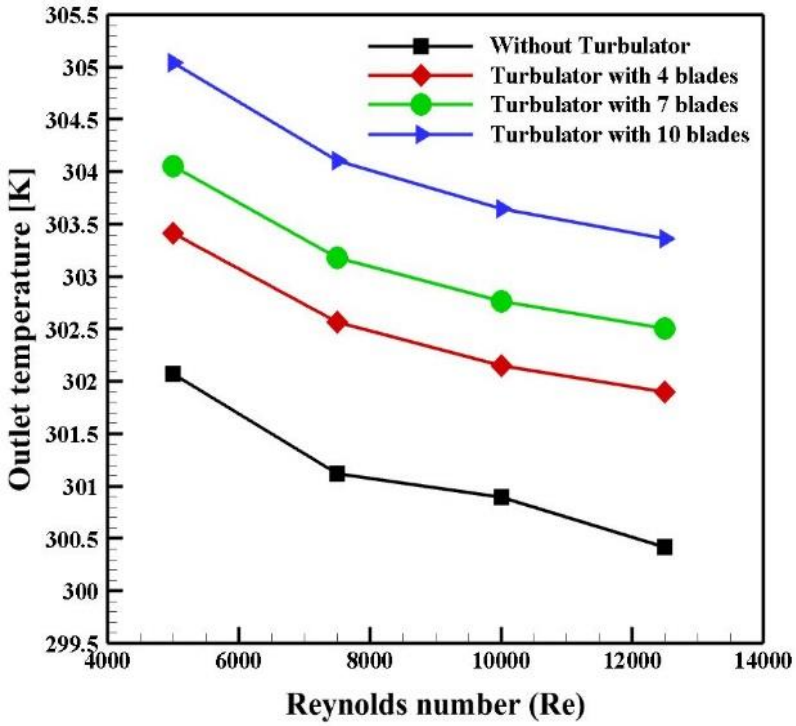

Figure 6 Outlet temperature versus Reynolds number for different turbulators.

Figure 7 depicts the variation in pressure drop with Reynolds number for different turbulator configurations and a plain tube. With increasing Reynolds number, the pressure drop intensifies due to heightened shear stress from increased velocity. Across all Reynolds numbers, pressure drop values rise with greater numbers of turbulator blades, mainly due to increased surface area.

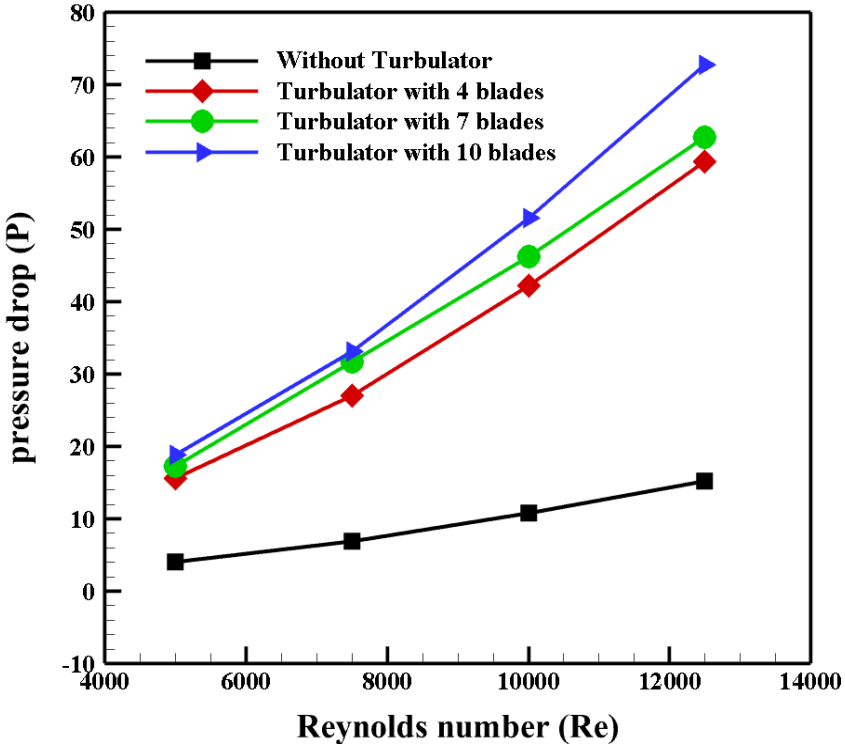

Figure 7 Pressure drop as a function of Reynolds number for various turbulators.

4.2 The Effect of Nanofluids

Figure 8 illustrates the relationship between the heat transfer coefficient and Reynolds number (Re). The graph shows that the heat transfer coefficient increases with Reynolds number, especially at a specific volume concentration of nanoparticles. Notably, among the studied nanofluids, the hybrid SWCNT-CuO/water nanofluid demonstrates superior thermal performance compared to both CuO/water and SWCNT/water nanofluids.

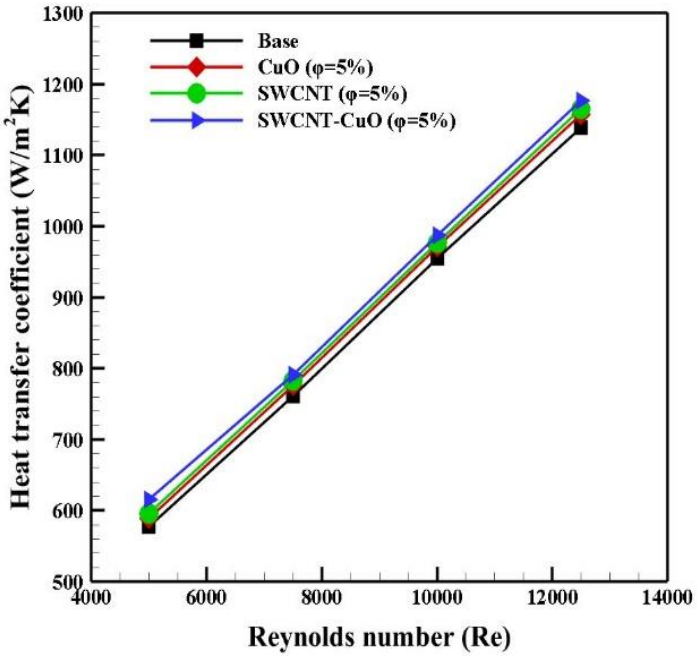

Figure 8 Variation of heat transfer coefficient with Reynolds number for different heat transfer fluids.

Additionally, Figure 9 demonstrates that at a constant Reynolds number, the heat transfer coefficient increases with higher volume concentrations of nanoparticles. This trend is linked to the thinning of the thermal boundary layer as the Reynolds number rises. Moreover, increasing the volume concentration of nanofluid enhances its thermal conductivity, thereby further augmenting the heat transfer coefficient.

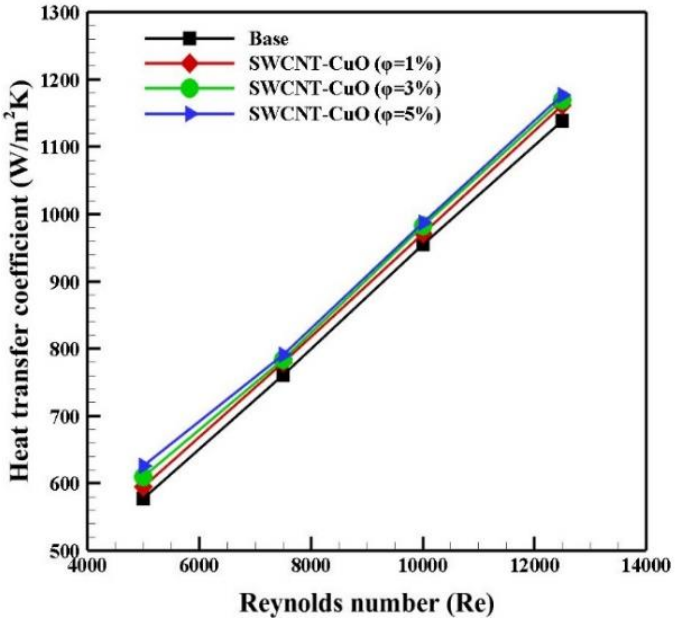

Figure 9 Heat transfer coefficient as a function of Reynolds number for various concentrations of hybrid nanofluid.

Figure 10 demonstrates the outlet temperature in terms of Reynolds number at different volume concentrations of hybrid nanofluids for the collector with a 10-blade turbulator. As the Reynolds number enhanced, the outlet temperature reduced but at a constant value of the Reynolds number, the outlet temperature increased with the volume concentration of nanoparticles. Raising the volume concentration of nanofluid improves its thermal conductivity, leading to increased energy exchange via molecular diffusion. Nonetheless, at higher inlet velocities, the reduced duration of heat transfer between the working fluid and hot surface causes a decline in outlet temperature, despite the higher heat transfer coefficient achieved at higher Reynolds numbers.

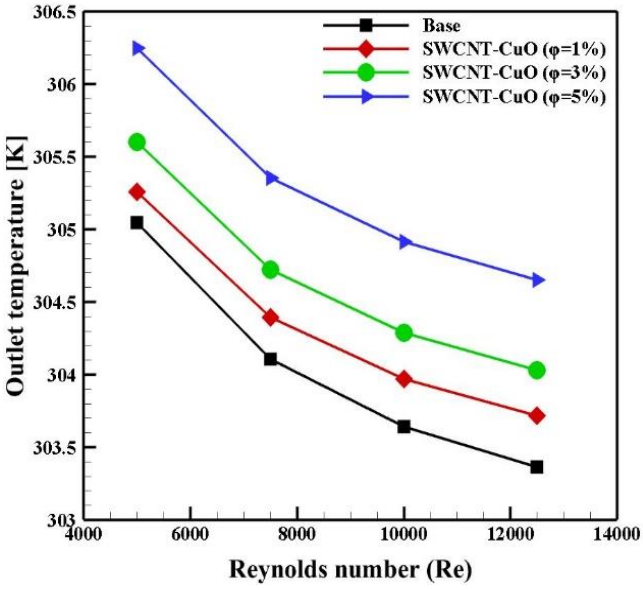

Figure 10 Variation of outlet temperature with Reynolds number for various concentrations of hybrid nanofluid.

Figure 11 depicts the variation in pressure drop with Reynolds number for different volume concentrations of hybrid nanofluid in a collector equipped with a 10-blade turbulator. At consistent Reynolds numbers, pressure drop increases with higher volume concentrations. This effect is attributed to increased nanofluid viscosity due to volume concentration. The maximum pressure drop change is observed to be 44% at a Reynolds number of 5000 and a volume fraction of 5%, compared to the base fluid.

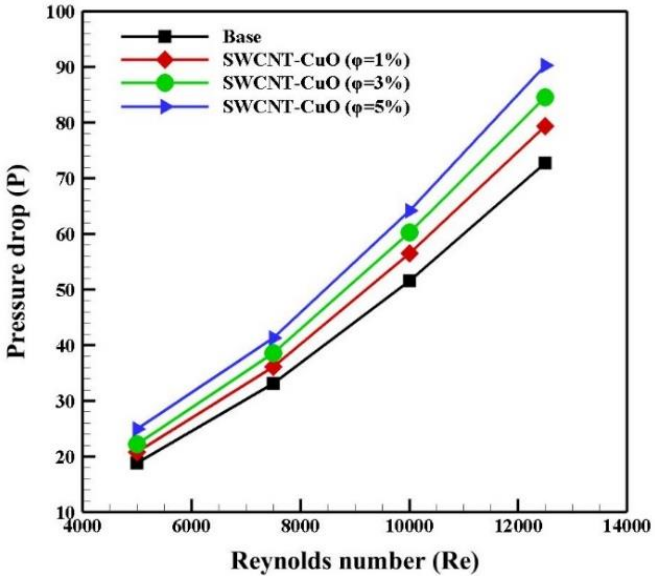

Figure 11 Pressure drop as a function of Reynolds number for various turbulators.

In Figure 12, the changes in Performance Evaluation Criteria (PEC) with Reynolds number are shown for various volume concentrations of nanoparticles in a collector featuring a 10-blade turbulator. As the Reynolds number increases, there are cases where the PEC (Performance Evaluation Criterion) increases, while in others, it decreases. This fluctuation is attributed to the simultaneous effects of two factors: the augmentation of bulk motion in the nanofluid and the rise in shear stress resulting from an increase in velocity gradient due to higher Reynolds numbers. The increase in Reynolds number generally leads to enhanced heat transfer coefficients but also results in heightened friction coefficients, contributing to the fluctuation in the PEC.

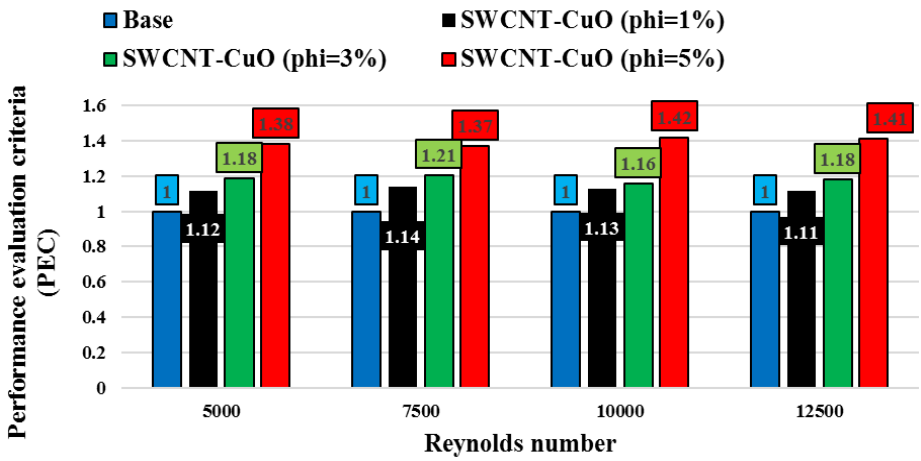

Figure 12 Pressure drop as a function of Reynolds number for various turbulators.

Moreover, with increasing volume concentration of nanoparticles, the PEC improves across all Reynolds numbers. This improvement is due to the heightened thermal conductivity and viscosity of the nanofluid resulting from the increased volume concentration. In this study, the positive impact of enhanced thermal conductivity outweighs the negative impact of increased dynamic viscosity, resulting in an overall enhancement of the PEC with volume concentration.

5. Conclusions

This study comprehensively investigated the thermal-hydraulic performance of parabolic trough collectors (PTCs) enhanced with three configurations of fin-spiral turbulators (4, 7, and 10 blades) and water-based nanofluids, including single-walled carbon nanotubes (SWCNT), cupric oxide (CuO), and a hybrid SWCNT-CuO composition. Simulations were performed for Reynolds numbers ranging from 5000 to 12,500 and nanofluid volume concentrations of 1%, 3%, and 5%.

The key findings are as follows:

- The inclusion of turbulators significantly enhanced heat transfer. Specifically, the 10-blade turbulator achieved a 12.25% improvement in the heat transfer coefficient compared to a plain tube, while the 7-blade and 4-blade turbulators showed improvements of 9.8% and 6.7%, respectively.
- Among the tested nanofluids, the hybrid SWCNT-CuO/water demonstrated superior thermal performance, with a 24.8% increase in thermal conductivity compared to the base fluid and an 8.5% improvement over CuO/water.
- The maximum pressure drop occurred with the hybrid nanofluid at 5% volume concentration, showing an increase of 44% compared to the base fluid. Despite this, the Performance Evaluation Criterion (PEC) for the hybrid nanofluid improved by 15.6% compared to CuO/water, highlighting its efficiency in balancing heat transfer enhancement with flow resistance.

The novelty of this study lies in the combined application of fin-spiral turbulators and hybrid nanofluids, which has not been extensively explored in the literature. The findings contribute to advancing the design of PTCs by demonstrating a hybrid approach that simultaneously enhances thermal efficiency and system performance. This work provides valuable insights for optimizing PTC systems and offers a foundation for future research on integrating advanced geometries and nanofluids to further improve solar thermal systems.

6. Future Research Work

While this study offers significant insights into the thermal-hydraulic performance of parabolic trough collectors (PTCs) enhanced with fin-spiral turbulators and hybrid nanofluids, certain limitations should be acknowledged. The numerical simulations, based on the Standard k-ε turbulence model, require further experimental validation to confirm the findings under varying operating conditions. Additionally, the long-term stability and dispersion characteristics of the hybrid SWCNT-CuO nanofluid were assumed and should be experimentally verified to address issues like sedimentation and thermal degradation. Although pressure drop effects were analyzed, a detailed cost analysis of implementing hybrid nanofluids and advanced turbulators in PTC systems was not included and should be explored in future studies. Furthermore, the turbulator configurations analyzed were limited to specific geometries, and investigating alternative designs,

such as twisted or perforated turbulators, could provide additional optimization opportunities. Similarly, only three nanofluid compositions were evaluated, highlighting the need to explore other hybrid nanofluids with varying ratios or nanoparticles. To address these limitations, future research should focus on experimental validation of the numerical results, transient simulations under dynamic operating conditions, and the use of advanced turbulence models like Large Eddy Simulation (LES) for improved accuracy. Additionally, economic and environmental impacts of these enhancements should be assessed, along with the integration of optimized PTCs with thermal energy storage systems to further improve energy efficiency.

Nomenclature

ρ	density	(kg/m^3)
c_p	heat capacity	(kJ/kg.K)
λ	thermal conductivity	(W/m.K)
P	pressure	(N/m^2)
T	temperature	(K)
u	velocity	(m/s)
φ	Nanoparticle concentration	-
μ	Viscosity	(Pa.s)
k	Turbulent kinetic energy	(J/kg)
ε	Turbulence dissipation	(J/kg.s)
S_r	source term	(W/m^3)
L	length	(m)
D	diameter	(m)
q	heat flux	(W/m^2)
Nu	Nusselt number	-
Re	Reynolds number	-
f	Friction factor	-

Abbreviations

PTC	parabolic trough collector
HTC	heat transfer coefficient
TKE	turbulence kinetic energy
UDF	user-defined function
PEC	performance evaluation criterion
ANU	average Nusselt number
SWCNT	Single-wall carbon nanotubes
PV	photovoltaic

Subscripts

f	base fluid
nf	nanofluid
hnf	hybrid nanofluid

s solid particle

Acknowledgments

The authors gratefully acknowledge support from the Industrial Training and Assessment Center (ITAC) and the Center for Energy Systems Research at Tennessee Technological University.

Author Contributions

The authors confirm their contribution to the paper as follows: conceptualization, software, validation, and writing the original draft by Mohsen Pourfallah; Methodology, Investigation, and review and editing by Ethan Languri.

Funding

The authors declare that they have received no funding for this paper.

Competing Interests

The authors declare that they have no known competing financial interests or personal relationships that could have appeared to influence the work reported in this paper.

References

1. Falope T, Lao L, Hanak D, Huo D. Hybrid energy system integration and management for solar energy: A review. Energy Convers Manage. 2024; 21: 100527.
2. Zadeh MN, Pourfallah M, Sabet SS, Gholinia M, Mouloodi S, Ahangar AT. Performance assessment and optimization of a helical savonius wind turbine by modifying the Bach's section. SN Appl Sci. 2021; 3: 739.
3. Ikhwan M, Haditiar Y, Wafdan R, Ramli M, Muchlisin ZA, Rizal S. M2 tidal energy extraction in the Western Waters of Aceh, Indonesia. Renew Sustain Energy Rev. 2022; 159: 112220.
4. Atsu D, Seres I, Farkas I. The state of solar PV and performance analysis of different PV technologies grid-connected installations in Hungary. Renew Sustain Energy Rev. 2021; 141: 110808.
5. Hashemi SF, Pourfallah M, Gholinia M. Thermal performance enhancement in an indirect solar greenhouse dryer using helical fin under variable solar irradiation. Sol Energy. 2024; 267: 112217.
6. Araújo A, Ferreira AC, Oliveira C, Silva R, Pereira V. Optimization of collector area and storage volume in domestic solar water heating systems with on-off control-A thermal energy analysis based on a pre-specified system performance. Appl Therm Eng. 2023; 219: 119630.
7. Hadi M, Pourfallah M, Shaker B, Gholinia M, Ranjbar AA. Simulation of a solar power plant with parabolic receivers in several parts of Iran in the presence of latent heat thermal energy storage system. Therm Sci Eng Prog. 2022; 30: 101249.
8. Gobio-Thomas LB, Darwish M, Stojceska V. Review on the economic impacts of solar thermal power plants. Therm Sci Eng Prog. 2023; 46: 102224.

9. Shen Y, Jia B, Wang C, Yang W, Chen H. Numerical simulation of atmospheric transmittance between heliostats and heat receiver in tower-type solar thermal power station. Sol Energy. 2023; 265: 112107.
10. Singh D, Singh D, Mishra V, Kushwaha J, Dev R, Patel SK, et al. Sustainability issues of solar desalination hybrid systems integrated with heat exchangers for the production of drinking water: A review. Desalination. 2023; 566: 116930.
11. Aissa A, Qasem NA, Mourad A, Laidoudi H, Younis O, Guedri K, et al. A review of the enhancement of solar thermal collectors using nanofluids and turbulators. Appl Therm Eng. 2023; 220: 119663.
12. Sani FH, Pourfallah M, Gholinia M. The effect of MoS_2-Ag/H_2O hybrid nanofluid on improving the performance of a solar collector by placing wavy strips in the absorber tube. Case Stud Therm Eng. 2022; 30: 101760.
13. Sheikholeslami M, Farshad SA, Ebrahimpour Z, Said Z. Recent progress on flat plate solar collectors and photovoltaic systems in the presence of nanofluid: A review. J Clean Prod. 2021; 293: 126119.
14. Mashhadian A, Heyhat MM, Mahian O. Improving environmental performance of a direct absorption parabolic trough collector by using hybrid nanofluids. Energy Convers Manage. 2021; 244: 114450.
15. Abdulhaleem SM, Abed IM, Said NM, Abed AM. Numerical investigation of the effect of two-phase hybrid nanofluids on thermal-hydraulic performance and PEC of parabolic solar collectors. Eng Anal Bound Elem. 2023; 157: 12-20.
16. Dou L, Ding B, Zhang Q, Kou G, Mu M. Numerical investigation on the thermal performance of parabolic trough solar collector with synthetic oil/Cu nanofluids. Appl Therm Eng. 2023; 227: 120376.
17. Shaker B, Gholinia M, Pourfallah M, Ganji DD. CFD analysis of Al_2O_3-syltherm oil nanofluid on parabolic trough solar collector with a new flange-shaped turbulator model. Theor Appl Mech Lett. 2022; 12: 100323.
18. He Y, Geng Y, Guo S, Ma R, Li Z. A machine learning approach and numerical investigation for intelligent forecasting of entropy generation rate inside a turbulator-inserted solar collector tube. Eng Anal Bound Elem. 2024; 158: 375-384.
19. Negeed ES, Alhazmy M, Bokhary AY, Abulkhair H, Almas MA, Hedia HS. Numerical simulation of flat plate solar collector equipped with a turbulator containing water/copper-graphene hybrid nanofluid utilizing a two-phase model. Eng Anal Bound Elem. 2023; 156: 90-113.
20. Fuxi S, Sina N, Sajadi SM, Mahmoud MZ, Abdelrahman A, Aybar HŞ. Artificial neural network modeling to examine spring turbulators influence on parabolic solar collector effectiveness with hybrid nanofluids. Eng Anal Bound Elem. 2022; 143: 442-456.
21. Sheikholeslami M, Jafaryar M, Gerdroodbary MB, Alavi AH. Influence of novel turbulator on efficiency of solar collector system. Environ Technol Innov. 2022; 26: 102383.
22. Fang Y, Mansir IB, Shawabkeh A, Mohamed A, Emami F. Heat transfer, pressure drop, and economic analysis of a tube with a constant temperature equipped with semi-circular and teardrop-shaped turbulators. Case Stud Therm Eng. 2022; 33: 101955.
23. Babapour M, Akbarzadeh S, Valipour MS. An experimental investigation on the simultaneous effects of helically corrugated receiver and nanofluids in a parabolic trough collector. J Taiwan Inst Chem Eng. 2021; 128: 261-275.

24. Al-Aloosi W, Alaiwi Y, Hamzah H. Thermal performance analysis in a parabolic trough solar collector with a novel design of inserted fins. Case Stud Therm Eng. 2023; 49: 103378.
25. Dovom AR, Aghaei A, Joshaghani AH, Dezfulizadeh A. Numerical analysis of heating aerosol carbon nanofluid flow in a power plant recupesrator with considering ash fouling: A deep learning approach. Eng Anal Bound Elem. 2022; 141: 75-90.
26. Altunay FM, Pazarlıoğlu HK, Gürdal M, Tekir M, Arslan K, Gedik E. Thermal performance of Fe_3O_4/water nanofluid flow in a newly designed dimpled tube under the influence of non-uniform magnetic field. Int J Therm Sci. 2022; 179: 107651.
27. Sakhaei SA, Valipour MS. Thermal performance analysis of a flat plate solar collector by utilizing helically corrugated risers: An experimental study. Sol Energy. 2020; 207: 235-246.
28. Tavakoli M, Soufivand MR. Investigation of entropy generation, PEC, and efficiency of parabolic solar collector containing water/Al_2O_3-MWCNT hybrid nanofluid in the presence of finned and perforated twisted tape turbulators using a two-phase flow scheme. Eng Anal Bound Elem. 2023; 148: 324-335.
29. Bellos E, Tzivanidis C, Tsimpoukis D. Enhancing the performance of parabolic trough collectors using nanofluids and turbulators. Renew Sustain Energy Rev. 2018; 91: 358-375.
30. Khetib Y, Alzaed A, Alahmadi A, Cheraghian G, Sharifpur M. Application of hybrid nanofluid and a twisted turbulator in a parabolic solar trough collector: Energy and exergy models. Sustain Energy Technol Assess. 2022; 49: 101708.
31. Alnaqi AA, Alsarraf J, Al-Rashed AA. Hydrothermal effects of using two twisted tape inserts in a parabolic trough solar collector filled with MgO-MWCNT/thermal oil hybrid nanofluid. Sustain Energy Technol Assess. 2021; 47: 101331.
32. Wirz M, Petit J, Haselbacher A, Steinfeld A. Potential improvements in the optical and thermal efficiencies of parabolic trough concentrators. Sol Energy. 2014; 107: 398-414.
33. Mwesigye A, Bello-Ochende T, Meyer JP. Minimum entropy generation due to heat transfer and fluid friction in a parabolic trough receiver with non-uniform heat flux at different rim angles and concentration ratios. Energy. 2014; 73: 606-617.
34. Kazemipour S, Kabiri-Samani A, Asghari K. Numerical modelling of flow field at shaft spillways with the marguerite-shaped inlets. Proc Inst Civ Eng Water Manage. 2024; 177: 413-424.
35. He YL, Xiao J, Cheng ZD, Tao YB. A MCRT and FVM coupled simulation method for energy conversion process in parabolic trough solar collector. Renew Energy. 2011; 36: 976-985.
36. Mwesigye A, Meyer JP. Optimal thermal and thermodynamic performance of a solar parabolic trough receiver with different nanofluids and at different concentration ratios. Appl Energy. 2017; 193: 393-413.
37. Gholinia M, Moosavi SK, Pourfallah M, Gholinia S, Ganji DD. A numerical treatment of the TiO_2/$C_2H_6O_2$-H_2O hybrid base nanofluid inside a porous cavity under the impact of shape factor in MHD flow. Int J Ambient Energy. 2021; 42: 1815-1822.
38. Zou B, Dong J, Yao Y, Jiang Y. An experimental investigation on a small-sized parabolic trough solar collector for water heating in cold areas. Appl Energy. 2016; 163: 396-407.
39. Zhu X, Zhu L, Zhao J. Wavy-tape insert designed for managing highly concentrated solar energy on absorber tube of parabolic trough receiver. Energy. 2017; 141: 1146-1155.